Energy xxx (2014) 1–12

Contents lists available at ScienceDirect

Energy

journal homepage: www.elsevier.com/locate/energy

Thermoelectric generation coupling methanol steam reforming characteristic in microreactor

Feng Wang [a, *], Yiding Cao [b], Guoqiang Wang [c]

[a] Key Laboratory of Low-grade Energy Utilization Technologies and Systems (Chongqing University), Ministry of Education, Chongqing 400030, PR China
[b] Department of Mechanical and Materials Engineering, Florida International University, Miami, FL 33174, United States
[c] College of Power Engineering, Chongqing University, Chongqing 400030, PR China

ARTICLE INFO

Article history:
Received 23 July 2014
Received in revised form
17 October 2014
Accepted 5 December 2014
Available online xxx

Keywords:
Thermoelectric
Endothermic steam reforming
Hydrogen production
Cold spot
Microreactor

ABSTRACT

Thermoelectric (TE) generator converts heat to electric energy by thermoelectric material. However, heat removal on the cold side of the generator represents a serious challenge. To address this problem and for improved energy conversion, a thermoelectric generation process coupled with methanol steam reforming (SR) for hydrogen production is designed and analyzed in this paper. Experimental study on the cold spot character in a micro-reactor with monolayer catalyst bed is first carried out to understand the endothermic nature of the reforming as the thermoelectric cold side. A novel methanol steam reforming micro-reactor heated by waste heat or methanol catalytic combustion for hydrogen production coupled with a thermoelectric generation module is then simulated. Results show that the cold spot effect exists in the catalyst bed under all conditions, and the associated temperature difference first increases and then decreases with the inlet temperature. In the micro-reactor, the temperature difference between the reforming and heating channel outlets decreases rapidly with an increase in thermoelectric material's conductivity coefficient. However, methanol conversion at the reforming outlet is mainly affected by the reactor inlet temperature; while at the combustion outlet, it is mainly affected by the reactor inlet velocity. Due to the strong endothermic effect of the methanol steam reforming, heat supply of both kinds cannot balance the heat needed at reactor local areas, resulting in the cold spot at the reactor inlet. When the temperature difference between the thermoelectric module's hot and cold sides is 22 K, the generator can achieve an output voltage of 55 mV. The corresponding molar fraction of hydrogen can reach about 62.6%, which corresponds to methanol conversion rate of 72.6%.

1. Introduction

Thermoelectric (TE) generation is a static electricity generation method which converts heat energy to electric energy by a thermoelectric material. Heat sources of this method are very broad, including waste heat from industries, automobiles, fuel cells, marine engines and solar energy. Thermoelectric module creates voltage when there is a temperature difference between its cold and hot sides. Therefore, output power is in direct proportion to the temperature difference across the generator [1–5]. According to many studies on the thermoelectric generation, the key measures to improve efficiency of the power generation lie in the removal of the heat on the cold side of the module. Cooling methods of natural convection, air cooling, or water cooling has been adopted by researchers to remove the heat. However, these methods are either passive heat dissipation or active cooling with low cooling efficiency [6–10]. In this paper, an innovative cooling method is used by adopting the strong endothermic reaction of methanol steam reforming as the heat sink on the cold side of the thermoelectric module.

Fuel (such as methanol) steam reforming for hydrogen production is a strong endothermic process, in which a temperature difference between the reforming channel and heating channel always exists due to the heat transfer resistance when an external heat source is supplied [11–15]. This temperature difference between the two channels can be harnessed to generate electricity by coupling a thermoelectric generator in the process of heat transferring from the heating channel with the reforming channel [16,17]. Furthermore, low grade exhausted or waste heat with a temperature usually higher than 200 °C is widely available in

* Corresponding author. Tel.: +86013618203569.
E-mail address: wangfeng@cqu.edu.cn (F. Wang).

http://dx.doi.org/10.1016/j.energy.2014.12.019
0360-5442/

industrial furnaces, engine exhaust, and metallurgy. The heat capacity of the exhausted or waste heat resource in various industries may represent about 17% ~ 67% of the total fuel consumption [18,19]. Therefore recycling the waste heat energy may contribute to energy saving and emission reduction strategy of the global society [20,21]. Different temperatures and temperature difference distributions and their characters in reforming channel and heating channel under different intensity of the heat sources have been examined [22–24]. However, the studies focus mainly on catalyst preparation and optimization [25–28], and the study of the reaction heat effect especially cold spot character on the reactor catalyst bed is limited [29–34]. Additionally, there is no study on thermoelectric power generation coupling endothermic steam reforming as heat sink for hydrogen production in micro-reactors.

Therefore, in this paper a coupling process of thermoelectric generation and methanol steam reforming for hydrogen production is designed and analyzed. Firstly, a monolayer catalyst bed of CuO/ZnO/Al_2O_3 is packed in a micro-reactor to study its endothermic nature and cold spot phenomena in methanol steam reforming process. Effects of inlet reactant temperatures on the reforming products composition and methanol conversion are investigated. Variation of the cold spot with inlet temperature is also inspected. Then simulated waste heat and catalytic combustion are used as heat supply sources for the strong endothermic methanol steam reforming reaction coupling thermoelectric generation. Through this design, the grade of methanol is improved, and simultaneously CO_2 in the reaction system is removed, achieving the goal of improving fuel efficiency and reducing emissions in one system [35–37]. Characteristic of this coupling process is also studied by numerical simulation.

2. Cold spot characteristic of methanol steam reforming in micro-reactor

2.1. Micro-reactor design and experimental system

Experiments of methanol steam reforming for hydrogen production are carried out in a self-designed micro-reactor that is integrated with reactant preheating, gasification, overheating and reaction in one unit, as shown in Fig. 1. The reactor is heated by electric heaters. The dimensions of the reaction volume are 50 mm × 60 mm × 3.5 mm, which has a designed area slightly larger than that of the thermoelectric module. A monolayer catalyst bed is designed and packed in it. The catalyst particles used are of the shape of cylinder with a diameter of 5 mm and a height of 3.5 mm, which is prepared specifically to exactly match the reaction dimension. The type of the catalyst is commercial CuO/ZnO/Al_2O_3 catalyst with a total mass of 4.7 g. Inlet temperature T_{in} before reaction and reaction temperature T in catalyst bed are measured separately. T_{in} is regarded as the temperature of the reactant gas before it enters the reaction section, which is calculated as the

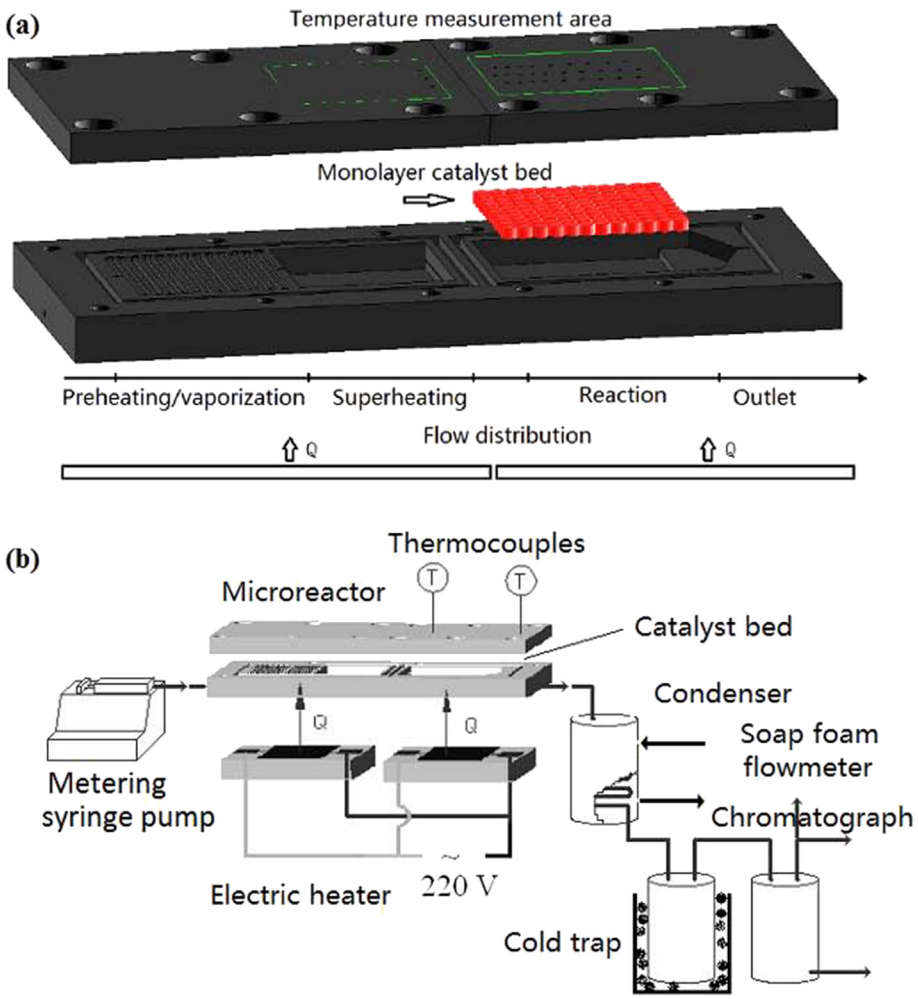

Fig. 1. Micro-reactor and experimental system for methanol steam reforming.

Please cite this article in press as: Wang F, et al., Thermoelectric generation coupling methanol steam reforming characteristic in microreactor, Energy (2014), http://dx.doi.org/10.1016/j.energy.2014.12.019

average value of the three measurement points in the preheating section as shown in Fig. 1.

The methanol used is analysis pure with a concentration greater than 99.5%. De-ionized water is prepared by using an ultrapure water machine dedicated for laboratory. In this paper, methanol and water molar ratio is set to 1.3. The reactant is injected into the system by the metering syringe pump. Before sampling, the experiment system has been operated for about 2 h to achieve a stable state. The products of methanol steam reforming are then passing through a condenser and a cold trap to gather un-reacted methanol and water. Finally the gas and un-reacted liquid products are analyzed by a gas chromatograph (GC-3000) equipped with a TDX-01 column and a Poropak-Q detector using helium as the carrier gas. Chromatography workstation is used to control the sampling process and to process data. Since a stainless steel material does not show any catalysis to this reaction, blank test of the stainless steel micro-reactor has not been carried out.

2.2. Performance of the micro-reactor

Since temperature has an important influence on methanol steam reforming process, effects of the inlet temperature T_{in} on reactor performance have been studied firstly and the results are shown in Fig. 2(a) and (b) at a reactant flow rate of 1.1 mol/min. The methanol conversion rate X_{CH_3OH} and H_2 production rate M_{H_2} increase almost linearly with the rising of T_{in}, but the highest methanol conversion rate at 280 °C is still less than 30% (Fig. 2(a)). One reason leading to this low methanol conversion may be that the flow rate of the reactant is too large for this condition and a large amount of the reactant follows out of the reactor without effective reaction, as the contact time of the reactant with the catalyst particle surface is too short. This conclusion may be verified from the results in Fig. 2 (c) and (d) at a lower reactant flow rate of 0.57 ml/min. Since the inlet reactant flow rate is decreased to 0.57 ml/min, methanol conversion increases to about 40% even at a relatively lower inlet temperature of 200 °C. Because of an extended residence time in the reactor, the reactant has longer, sufficient time to react on the catalyst surface.

At a lower reactant flow rate, the rate of H_2 production M_{H_2} experiences a similar variation to that of X_{CH_3OH}, and maximum M_{H_2} reaches 311 ml/min. However, H_2 molar fraction, F_{H_2}, and CO_2 selectivity, S_{CO2}, in the products decrease with the increasing of the inlet temperature. It has been established that with the increasing of reaction temperature of the methanol steam reforming reaction, more CO will be generated from methanol decomposition reaction pathway [11]. Therefore CO_2 selectivity from methanol steam reforming decreases and at the same time H_2 concentration drops.

However, at the inlet reactant flow rate of 0.57 ml/min, change of X_{CH_3OH} with T_{in} presents a "S" a shape as shown in Fig. 2(c), which is quite different from that of the higher inlet flow rate of 1.10 ml/min. As for H_2 molar fraction F_{H_2}, it increases gradually with inlet temperature, which shows a different variation on the contrary to the higher flow rate condition. The general trends of S_{CO_2} and F_{CO_2} are gradually decline with inlet temperature, which are in inverse variation with F_{CO}, indicating that methanol decomposition pathway in the system plays a more and more important role with an increase in T_{in} at a low reactant flow rate. Furthermore, the controlled process or step may be transformed with the variation of reactor inlet parameters.

2.3. Cold spot character of methanol steam reforming in microreactor

Different variations of the outlet parameters with the inlet temperature at reactant flow rates of 1.10 and 0.57 ml/min illustrate that heat and mass transfer processes may affect the reaction process of methanol reforming and associated reaction mechanism. The endothermic character of the reaction may be changed due to that reason. Therefore, the effect of temperature distribution on the microreactor monolayer catalyst bed has been studied and results are shown in Fig. 3. For all inlet temperatures of T_{in}, "cold spot" formed at the inlet region of the catalyst bed. Distribution of the

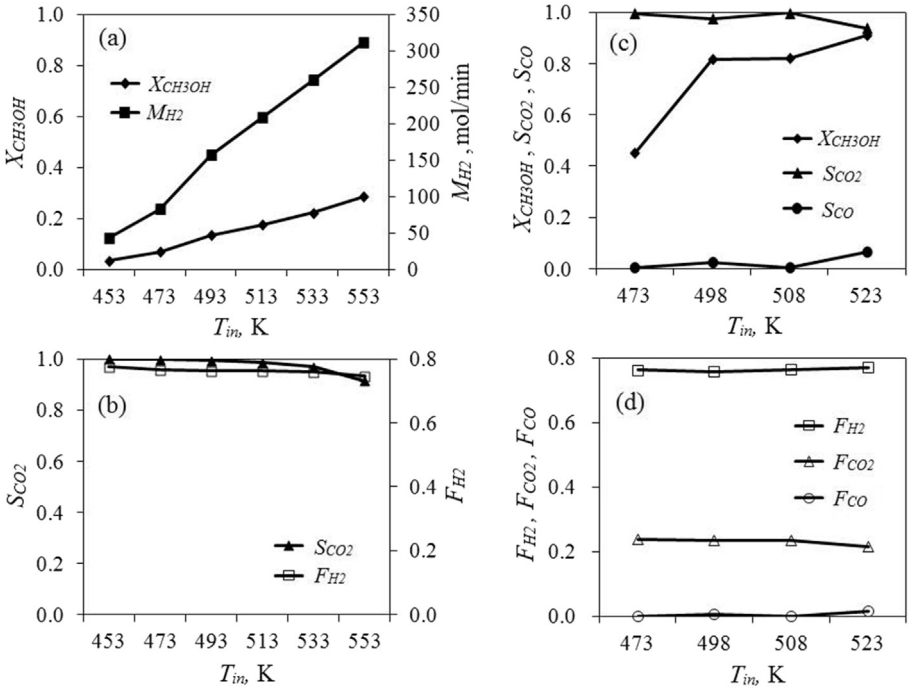

Fig. 2. Variation of reactor outlet parameters with T_{in}.

Please cite this article in press as: Wang F, et al., Thermoelectric generation coupling methanol steam reforming characteristic in microreactor, Energy (2014), http://dx.doi.org/10.1016/j.energy.2014.12.019

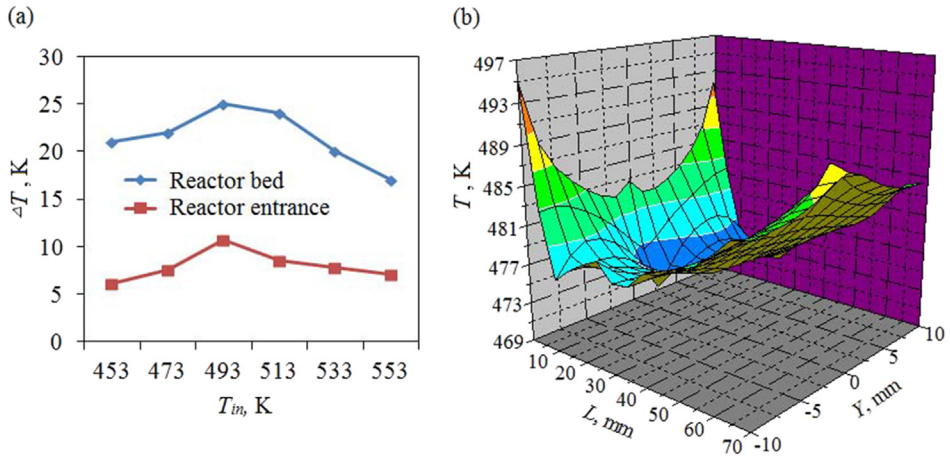

Fig. 3. (a) Change of temperature difference ΔT with T_{in}; (b) Temperature distribution in catalyst bed at T_{in} = 493 K.

temperature along the flow direction is that it decreases from the value of T_{in} to the value of the lowest cold spot temperature at a position of about 5 mm–10 mm away from the catalyst bed inlet, and then it increases to about the value of inlet temperature again. Furthermore, along the direction in width at the inlet section, the temperature is lower at the middle than that at the both sides of catalyst bed. The temperature difference is the biggest between the lowest cold spot temperature and that of the inlet temperature, leading to a higher heat transfer driving force compared with that of both sides.

At a higher inlet reactant flow rate, reactant concentration in the reaction area is relatively higher than that of the lower inlet reactant flow rate condition. Therefore the kinetics driving force due to the reactant concentration of methanol reforming reaction is larger at higher reactant flow rate. The total amount of reactant consumed is accordingly greater, which results in a larger heat sink in the reaction region. Finally the average temperature of the total reaction area drops, forming a heat transfer limitation from the bottom of the reactor inner surface to the catalyst bed at local areas. Poor heat transfer effect of the catalyst bed with larger catalyst particles intensifies this heat transfer limitation, especially in the middle of the inlet catalyst bed where the intensity of reaction is the highest. For the lower inlet reactant flow rate of 0.57 ml/min, cold spot effect is not obvious. Residence time of the reactant in the catalyst bed is longer but the total amount of consumed reactant may be less, so at the same heating condition, heat transfer limitation effect is small.

The maximum temperature differences, ΔT, over the total reactor catalyst bed and at the reactor inlet regions have been compared as presented in Fig. 3. It can be seen that both of the temperature differences experience a variation of increasing at first and then descending with the inlet temperature. However, the value of ΔT in the total reactor bed is larger than that at the reactor entrance. The maximum values of ΔT appear at the condition of inlet temperature of T_{in} = 220 °C. So it can be inferred that the inlet temperature of 220 °C is approximately the optimum reaction temperature of methanol steam reforming on copper based catalyst, which agrees with some other research work [38–40]. At this condition, the effect of heat absorption by endothermic methanol steam reforming reaches its strongest state, leading to a cold spot temperature difference of about 25 °C and 11 °C, respectively, for the total reactor bed and reactor entrance. As the heat transfer limitation is mainly caused by the poor thermal conductivity of the catalyst material, it is better to employ a coating catalyst rather than particle catalyst. Beyond that, the results of this paper may provide another solution for the cold spot effect in catalyst bed with strong heat effect reaction. For example, we can dilute the catalyst activity at a local cold spot region in the reactor, thus activity at that area will be decreased and so will the reaction intensity.

3. Characteristics of methanol steam reforming coupled with thermoelectric generation with heat source of simulated exhausted gas

3.1. Physical mathematical and kinetic model

According to the methanol steam reforming experiment results above, the coupling reactor model is designed and is shown in Fig. 4. It includes a methanol steam reforming channel, a simulated waste heat heating channel or methanol catalytic combustion channel, a thermoelectric generation module, and a middle partition.

The channel length of L is 40 mm, which is the size of the strong endothermic reaction region of the experiment system of the last section. The thermoelectric generation module has a height of H = 5 mm, and the steam reforming channel and heating channel have a height of h1 = 2 mm in order to enhance the heat and mass transfer by decreasing the reactor size. The thickness of the stainless steel partition, h2, is 1 mm. The size selection of the microreactor is based on the endothermic methanol reforming experimental results and available type of thermoelectric generator from on market with dimensions of 40 mm × 40 mm × 5 mm.

The reaction process in the methanol steam reforming channel has been established based on the following assumptions:

(1) Reactant gases are assumed to be ideal gases and the flow of the gas mixture in the channel is laminar and incompressible;
(2) Heat transfer by radiation of the fluid and the reaction channel surface is neglected due to the low reaction temperature;
(3) Gravitational and thickness effects of the catalytic layer are all neglected. Only surface reaction in the methanol steam reforming channel and methanol catalytic combustion channel has been considered; and
(4) In this reactor model, the catalyst used in reforming and catalytic combustion channels are assumed to be Cu-based and Pt-based catalytic coating, respectively, thus the corresponding reaction kinetics of methanol steam reforming and methanol catalytic combustion can be used in simulation;

Please cite this article in press as: Wang F, et al., Thermoelectric generation coupling methanol steam reforming characteristic in microreactor, Energy (2014), http://dx.doi.org/10.1016/j.energy.2014.12.019

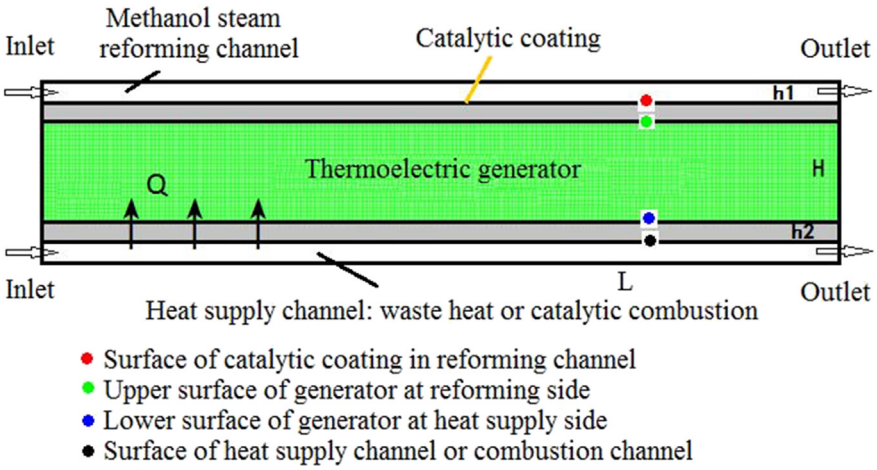

Fig. 4. Physical model of a methanol steam reforming coupled with thermoelectric generation.

The grids of the numerical model are uniform, quadrilateral grid structure, and the grid irrelevance has been inspected in order to eliminate grid density effect. The boundary conditions of the model are set as follows:

(1) Both boundaries of methanol steam reforming and hot air heating or catalytic methanol combustion heating inlets are VELOCITY-INLET boundaries; and the channel outlets are set as PRESSURE-OUTLET boundaries;
(2) Lower and upper boundaries of the model are set as SYMMETRICAL boundaries; and
(3) The other relevant sides are set as WALL boundaries.

Because the reaction fluid has been assumed to be ideal gas mixture in accordance with the Dalton law of partial pressure, the pressure of each component is in direct proportion to its mole fraction in the mixture. Ideal gas mixture enthalpy is the function of mass fraction of each component. Therefore process of methanol steam reforming channel can be described by a series of nonlinear partial differential equations for mass, momentum, energy and mass transfer of the components. Finally the governing equations are shown in the following.

Mass balance:

$$\frac{\partial}{\partial x_j}(\rho u_j) = 0 \tag{1}$$

Momentum balance:

$$\frac{\partial}{\partial x_j}(\rho u_j u_i) = -\frac{\partial p}{\partial x_i} + \frac{\partial}{\partial x_j}\left[\left(\mu\frac{\partial u_i}{\partial x_j} + \frac{\partial u_j}{x_i}\right)\right] \tag{2}$$

Energy balance:

$$\rho u_j \frac{\partial T}{\partial x_j} = \frac{\partial}{\partial x_j}\left(\frac{\lambda}{C_p}\frac{\partial T}{\partial x_j}\right) + R_T \tag{3}$$

At every point in channel space: $R_T = 0$, and on the catalytic surface, R_T satisfies the following relation:

$$R_T = \left(\sum_{i=1}^{2} r_i Q_i\right) \Big/ C_p \tag{4}$$

Here, r_i represents the reaction rate of methanol steam reforming or methanol catalytic combustion in the kinetic models. Q_i is the reaction heat in rate models.

Component conservation equation:

$$\rho u_j \frac{\partial Y_s}{\partial x_j} = \frac{\partial}{\partial x_j}\left(D\rho\frac{\partial Y_s}{\partial x_j}\right) + R_s \tag{5}$$

where R_s is the consumption rate of the methanol, and $R_s = 0$ at every point in the channel space; on the catalytic surface, it satisfies the following equation:

$$R_s = r_i M_s \tag{6}$$

where M_s is the mass fraction of component s.

Ideal gas law:

$$p = \rho R_g T \sum \frac{Y_s}{M_s} \tag{7}$$

Closure equation: the sum of mass fraction for all the component is unity:

$$\sum Y_s = 1 \tag{8}$$

In the above equations, p, ρ, u, μ, D, and λ are pressure, density, velocity, viscosity, diffusion coefficient, and thermal conductivity, respectively. R_g is the gas constant; T is temperature; q is the heat of reaction. Y_s, M_s *and* R_s are the mass fraction, mole weight, and generation/consumption rate of species s, respectively.

With the application of a 2D constant solver in CFD software of FLUENT, the numerical solutions are obtained. Laminar flow and general finite reaction rate model have been applied. Specific heat capacity at constant pressure, thermal conductivity, and viscosity of the gas mixture fluid has been calculated by weighted average of the ideal gas components. Quality diffusion coefficient is set to 2.88×10^{-5} m^2/s.

Hot air is used to simulate the waste and exhausted heating medium. Because there is no reaction, only fluid flow and heat transfer equations are considered in the heating channel. Inlet velocity in the heating channel is set to that of the reforming channel. Three catalytic reactions of steam reforming (SR), methanol decomposing (DE), water gas shift reaction (WGS) may be involved in the reforming reaction system. Research shows that outlet CO content is very small on a copper based catalyst in methanol steam reforming for hydrogen production [11]. Therefore, single rate kinetic model of methanol reacting with water (SR) is applied for this process. Then rate of methanol steam reforming reaction r_{SR} (mol/(g h)) can be simplified to the fowling power law function [41].

Please cite this article in press as: Wang F, et al., Thermoelectric generation coupling methanol steam reforming characteristic in microreactor, Energy (2014), http://dx.doi.org/10.1016/j.energy.2014.12.019

$$r_{SR} = 1.20 \times 10^7 \exp\left(-96240 \Big/ \left(RT\right)\right) C_{CH_3OH}^{0.60} C_{H_2O}^{0.45} \quad (9)$$

For methanol catalytic combustion reaction rate, r_{MC} (mol/(g h)) can be simplified to the fowling power law function [42].

$$r_{MC} = 4.42 \times 10^8 \exp\left(-32600 \Big/ \left(RT\right)\right) C_{CH_3OH}^{0.5} \quad (10)$$

Effects of material conductivity on the thermoelectric generator, temperature and components distribution in the channel, and transport characteristics of the reactor are studied. Performance of the generator module is also predicted according to the experimental data.

3.2. Influence of conductivity and inlet parameter

According to the theory, the figure of merit of thermoelectric generation module is $Z = \alpha^2\sigma/\lambda_{TE}$, where α is the SEEBECK coefficient, σ is the electrical conductivity of the thermoelectric material, and λ is the associated effective thermal conductivity. If the other parameters are fixed, output power of the generator is reduced to a function of the effective thermal conductivity of the material, λ_{TE}. It is reasoned that the thermoelectric material effective thermal conductivity has a great effect on its performance as well as on the temperature difference between the module cold and hot sides. In this study, since the thermoelectric generator has been coupled to methanol steam reforming micro-reactor, λ_{TE} will also has important influence on the reactor performance. Reducing effective thermal conductivity requirement is one of the goals of research in the thermoelectric materials including P, N electric dipole materials. It is reported in literature that the effective thermal conductivity of applicable material is in the range of 0.01–10 W/(m K). Therefore, λ_{TE} of the generator module in this study is set from 0.01 to 10 W/(m K), and its influence at four different orders of magnitude has been simulated and analyzed, as shown in Fig. 5.

It can be seen from Fig. 5, when inlet velocity u_{in} is set to 1.5 m/s, the maximum temperature difference between methanol steam reforming channel and hot air heating channel outlets, ΔT, decreases rapidly with increasing of the effective thermal conductivity coefficient of thermoelectric material λ_{TE}. Especially when the effective conductivity coefficient is 10 W/(m K), the temperature difference ΔT is only about 2 K. Methanol conversion X_{CH_3OH} increases slightly with effective thermal conductivity coefficient of the module, but the total increment is very small. It is influenced much more by the inlet temperature T_{in}. At an inlet temperature of 473 K, methanol conversion is the lowest. With the increasing of the inlet temperature, X_{CH_3OH} rises. However, increment of the methanol conversion is very small when inlet temperature is over 573 K. Although overall output power of the thermoelectric generator with low temperature difference can be improved by series and parallel module additions, the above analysis shows that the reactor performance vs. the methanol conversion and the thermoelectric generator performance vs. increment can be improved at an inlet temperature above 523 K even if the material effective thermal conductivity coefficient is below the value of 0.1 W/(m K). Therefore the effective thermal conductivity coefficient of the thermoelectric generator material is set to 0.1 W/(m K) to study the influence of inlet parameters of u_{in} and T_{in} on methanol conversion X_{CH_3OH} and ΔT, and the results are shown in Fig. 6.

It can be seen in Fig. 6 that methanol conversion X_{CH_3OH} decreases with increasing of inlet velocity u_{in}, and increases with inlet temperature T_{in} in the steam reforming channel. However maximum temperature difference ΔT between the two channel outlets increases with inlet velocity, and the increment is larger at higher inlet temperatures. With the increase of the inlet temperature at the two channels, ΔT increases gradually. It indicates that although methanol conversion decreases at a higher inlet velocity, the total quantity of methanol converted increases with the inlet velocity. The heat absorbed also increases, thus forming a larger heat sink there, which intensifies the temperature difference between the steam reforming channel and heating channel outlets. Therefore, reforming reactor and generator performance should be considered simultaneously for methanol conversion and maximum temperature difference in the coupling model.

3.3. Temperature distribution and transport characteristics

As shown in Fig. 7, temperature distribution of the reactor for hydrogen production coupled with the thermoelectric generation model has been analyzed under the conditions of $\lambda_{TE} = 0.1$ W/(m K), $T_{in} = 573$ K and $u_{in} = 1.5$ m/s.

It can be seen that the temperature distribution along the surface of the catalytic coating in the reforming channel and that along the upper surface of the generator on the reforming side are similar. It is also similar for the surface of the heat supply channel and the lower surface of the generator on heat supply side. Both their temperatures gradually decrease along the fluid flow direction. Then a uniform temperature difference of about 20 K forms between the cold and hot side of the thermoelectric generation module. Since there exits an axial temperature difference along both channels due to heat transfer, the application of a good heat conductor, such as stainless steel, copper, or aluminum, on both sides of the thermal electric generation model can get a better temperature distribution at the hot and cold ends of the generator. It can be beneficial for improving the performance of power generation, as validated by the e experiment result of the thermoelectric module. When the temperature difference ΔT reaches

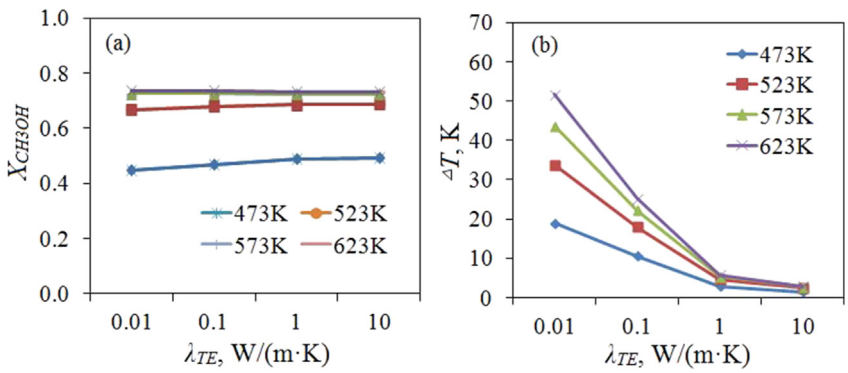

Fig. 5. Variation of methanol conversion X_{CH_3OH} and ΔT with effective thermal conductivity coefficient of thermoelectric material at different temperatures.

Please cite this article in press as: Wang F, et al., Thermoelectric generation coupling methanol steam reforming characteristic in microreactor, Energy (2014), http://dx.doi.org/10.1016/j.energy.2014.12.019

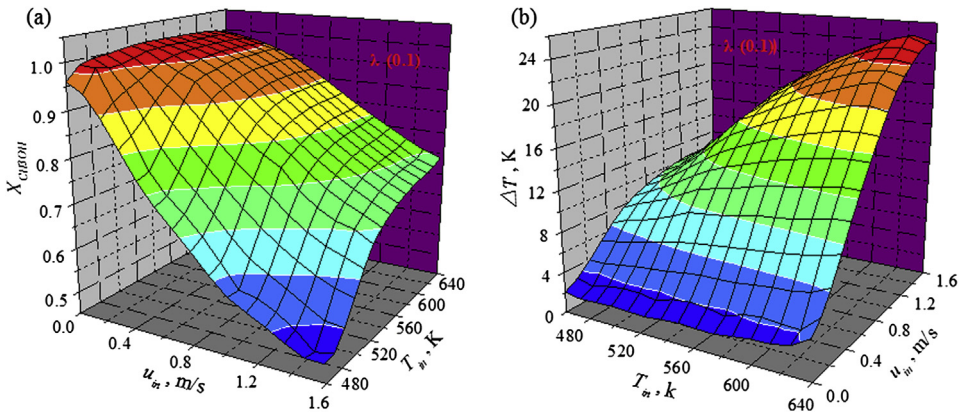

Fig. 6. Variation of methanol conversion (a) and largest temperature difference (b) with inlet velocity and temperature.

39.4 K, open circuit voltage of the thermoelectric generation module is 0.782 V with a temperature testing module on its both sides. While when the temperature testing module is taken out of the generator, the open circuit voltage of the thermoelectric generation module reaches 2.408 V. At the same time, good conductor material will also be helpful to reduce the cold spot effect in the steam reforming channel, and consequently to enhance the efficiency of hydrogen production.

Moreover, it can be seen that temperatures of the reforming channel and heating channel drop rapidly at the reactor inlet although the magnitudes of decrement are different. The temperature in the reforming channel on the catalysis surface drops rapidly from 573 K to 537 K, even lower than the temperature on the upper surface of the generator at reforming side. The strong heat absorption effect of the methanol steam reforming reaction results in a cold spot temperature difference at reactor inlet. Since energy density of exhausted or waste heat is low compared to that of the strong endothermic reaction, the cold spot effect cannot be removed completely. This can also be illustrated by the heat flux on the channel surfaces heated by waste heat and that of the methanol steam reforming, as shown in Fig. 8. Fig. 8 provides the heat fluxes on the surfaces of two channels in the reactor and up and down sides of the thermoelectric generation module under the condition of $\lambda_{TE} = 0.1$ W/(m K), $u_{in} = 1.5$ m/s, and $T_{in} = 573$ K.

Due to the strong endothermic effect of the methanol steam reforming, the heat flux on the inlet surface of the reforming channel is up to 1643 W/m^2. Driven by the temperature difference, the heat flux on the corresponding surface of heat supplying channel is up to 2304 W/m^2. The absolute value of the heat fluxes on the inner surfaces of the two channels decreases rapidly along the flow direction. Furthermore, the heat fluxes on the surfaces of the reforming and heating channels are always the same in the flow direction. It indicates that an axial temperature difference exists in the stainless steel material that is used as the contacting plates in the thermoelectric generation module. The stainless steel material has been proved to be useful in storing and even distributing heat.

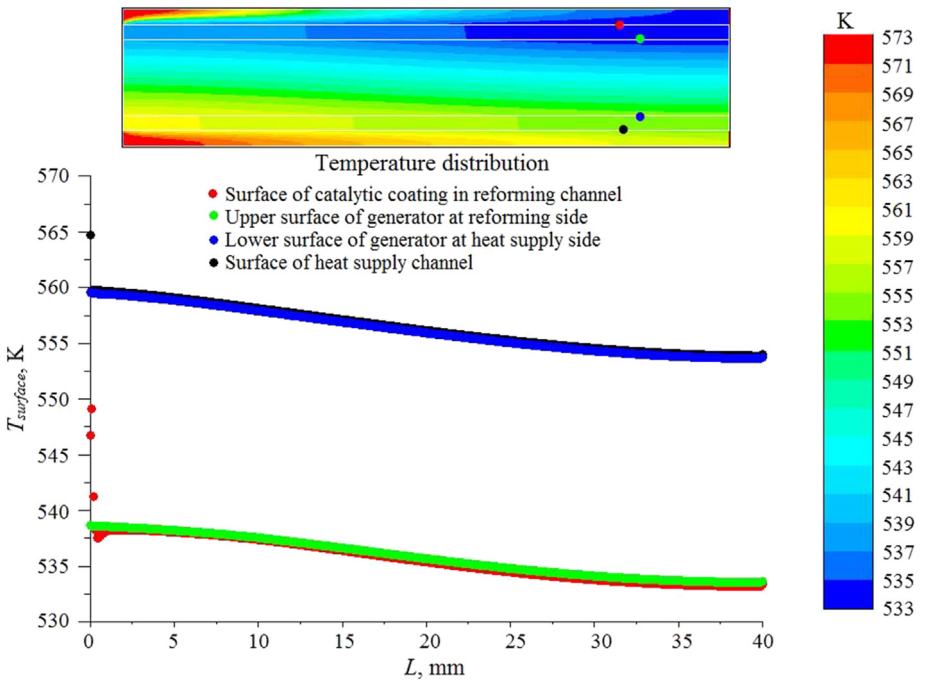

Fig. 7. Temperature contours in the reactor, on the surfaces of the methanol steam reforming and heat supplying channel, and up and down sides of the thermoelectric generation module.

Please cite this article in press as: Wang F, et al., Thermoelectric generation coupling methanol steam reforming characteristic in microreactor, Energy (2014), http://dx.doi.org/10.1016/j.energy.2014.12.019

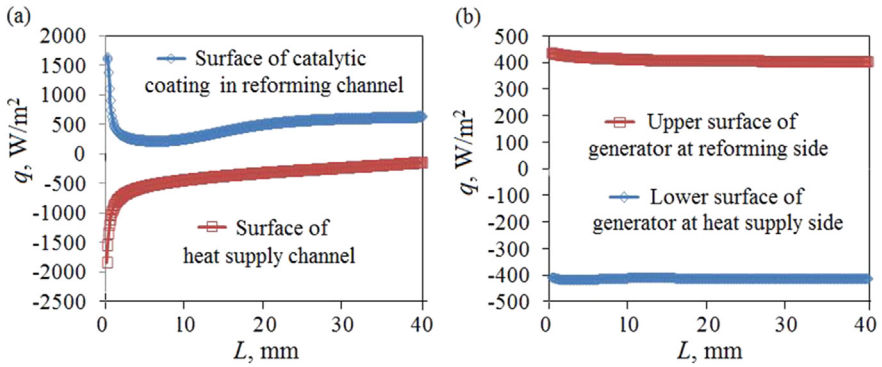

Fig. 8. Heat flux on the surfaces of the two channels in the reactor (a) and up and down sides of the thermoelectric generation module (b).

The heat flux on the upper surface of the generator at reforming side and that on the lower surface of the generator at heat supply side are almost the same.

3.4. Components distribution and performance prediction of the thermoelectric module

At conditions of $\lambda_{TE} = 0.1$ W/(m K), $T_{in} = 573$ K and $u_{in} = 1.5$ m/s, reactants and products mass fraction distributions along the centre line of the methanol steam reforming channel and on the surface near the reaction wall are investigated as shown in Fig. 9.

It can be seen that mass factions of reactants of CH_3OH and H_2O decrease gradually along the flowing direction along the reforming channel centre line. However, their distributions near the reaction surface along the reforming channel are very different; Mass factions of CH_3OH and H_2O decrease sharply in the inlet area of the reactor and then maintain almost the same all along the remaining reforming channel. This is an indication of the mass transport limitation from the reaction surface to the main stream, although the distance is only 1 mm. The mass fraction distributions of the products are on the contrary to the reactants, which increase along the reforming channel centre line sharply near the reaction surface along the flow direction. At the reforming channel outlet, molar fraction of hydrogen reaches about 62.6%, which corresponds to methanol conversion of 72.6%. Therefore, the scale of the reforming channel can be further reduced to get a higher mass transfer coefficient and subsequently a higher methanol conversion.

Performance of the thermoelectric module used in the simulation model has been tested. Nine thermocouple test points have been placed on the hot and cold sides of the generator as shown in Fig. 10. Temperature distributions on its both sides and temperature differences ΔT are also obtained. Temperature distribution on the hot side of the thermoelectric module is fairly uniform, but it is slightly uneven on the cold side. Since heat is transferred from the hot side to the cold side of the generator, it can be inferred that the effective thermal conductivity of the module varies slightly over the generator, which causes an uneven the temperature difference distribution. With the increasing of ΔT between the hot and cold sides of the module, the associated open circuit voltage increases as shown in Fig. 10. The maximum output power of a single thermoelectric module reaches 85 mW at the condition of $\Delta T = 34$ K. According to the test, when ΔT reaches the condition of about 22 K in the simulation of methanol steam reforming coupled with thermoelectric generation, open circuit voltage of the thermoelectric module reaches about 0.7 V. According to the theory, maximum output power of the simulation model with one thermoelectric generation module will reach 55 mW.

4. Characters of coupled methanol steam reforming and thermoelectric generation using heat source of methanol catalytic combustion

4.1. Influence of conductivity coefficient and inlet parameter

In this situation, methanol catalytic combustion is used as the heat source for thermoelectric generation. Effects of thermal the conductivity coefficient of the generator module varying from 0.01 to 10 W/(m K) have been analyzed as shown in Fig. 11.

As can be seen from Fig. 11, with a micro-reactor inlet velocity of $u_{in} = 1.5$ m/s, maximum temperature difference ΔT between methanol steam reforming outlet and catalyst combustion outlet decreases rapidly with the increasing of λ_{TE}. With an effective conductivity of 10 W/(m K), the temperature difference ΔT is about 3.4 K, which is slightly larger than that of the exhausted gas heat

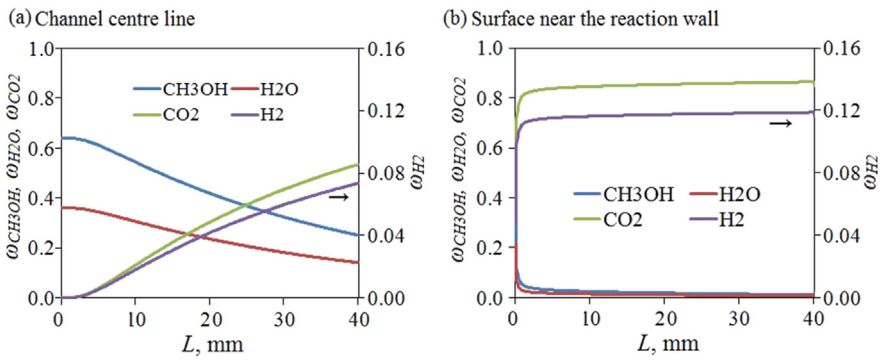

Fig. 9. Mass fraction of components in reforming channel along the centre line (a) and near the reaction wall (b).

Please cite this article in press as: Wang F, et al., Thermoelectric generation coupling methanol steam reforming characteristic in microreactor, Energy (2014), http://dx.doi.org/10.1016/j.energy.2014.12.019

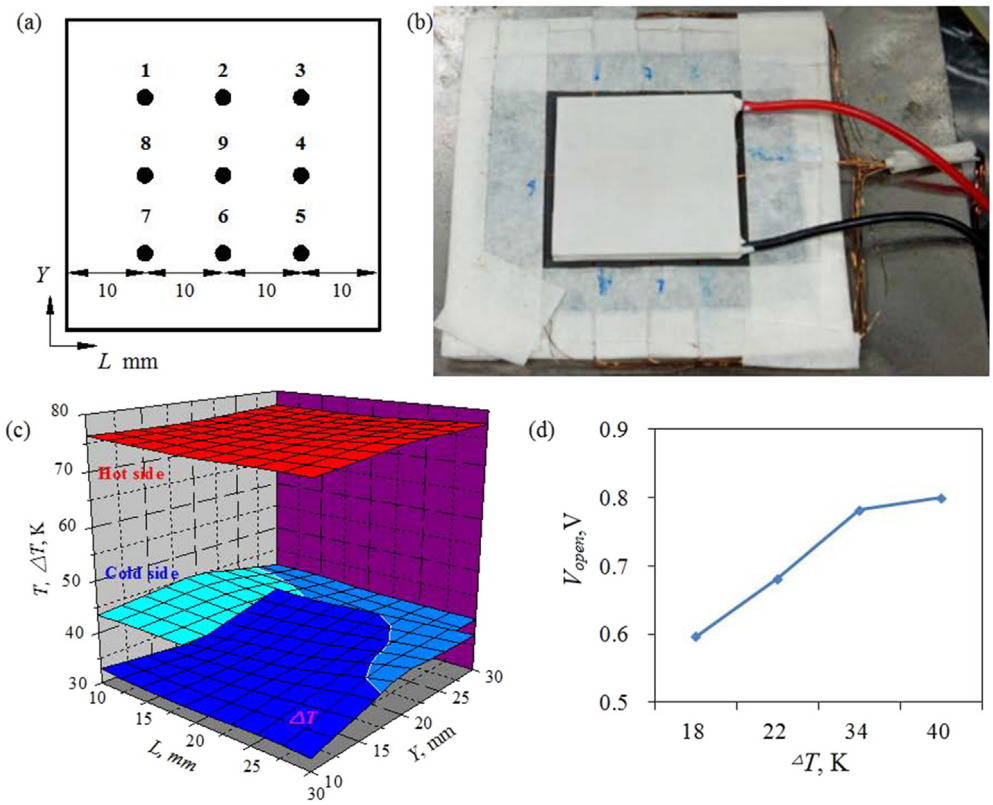

Fig. 10. Temperature measuring point layout on the thermoelectric module (a)and (b),Temperature and ΔT distributions on and between hot and cold sides of the thermoelectric module (c), and Variation of open circuit voltage with ΔT (d).

source condition. The lower the thermal conductivity, the bigger the maximum temperature difference ΔT at the reactor outlet and the greater the influence of the temperature. Methanol conversion $X_{CH_3OH}(SR)$ at the steam reforming outlet also increases slightly with λ_{TE} at the condition of lower inlet temperatures (T_{in} = 473 K, 523 K), but the total increment is very small. It even reverses the trend and goes down slightly at higher inlet temperatures (T_{in} = 573 K, 623 K). $X_{CH_3OH}(SR)$ is also influenced greatly by the inlet temperature T_{in}. At an inlet temperature of 473 K, the methanol conversion is the lowest. When the inlet temperature is greater than 573 K, the change of $X_{CH_3OH}(SR)$ levels off and approaches about 73%.

Methanol conversion (MC) at catalytic combustion channel outlet $X_{CH_3OH}(MC)$ is much higher than that of $X_{CH_3OH}(SR)$. It first increases with the increasing of λ_{TE} at lower inlet temperatures, but then decreases at higher inlet temperature with module effective thermal conductivity. The influence of T_{in} on $X_{CH_3OH}(MC)$ is smaller than that on $X_{CH_3OH}(SR)$. At module effective thermal conductivity of 0.01 W/(m K), $X_{CH_3OH}(MC)$ is about 86%. The highest value of conversion is 87% at higher module effective thermal conductivity. Similarly, λ_{TE} is fixed at a value of 0.1 W/(m K) to study the influence of inlet velocity u_{in} and temperature T_{in} on methanol conversion $X_{CH_3OH}(SR)$, $X_{CH_3OH}(MC)$ and ΔT. The results are shown in Fig. 12.

It can be seen in Fig. 12, methanol conversion $X_{CH_3OH}(SR)$ decreases with increasing of inlet velocity u_{in} since the contact time of the reactant with the catalyst surface is reduced. It increases with inlet temperature T_{in} in the steam reforming channel due to the enhancement of reaction rate. $X_{CH_3OH}(MC)$ also decreases with u_{in} on the catalytic combustion side. However, the influence of the inlet temperature on $X_{CH_3OH}(MC)$ is relatively small, which is consistent with the above analysis. This indicates that the heat source characteristics of the exothermic catalytic combustion is

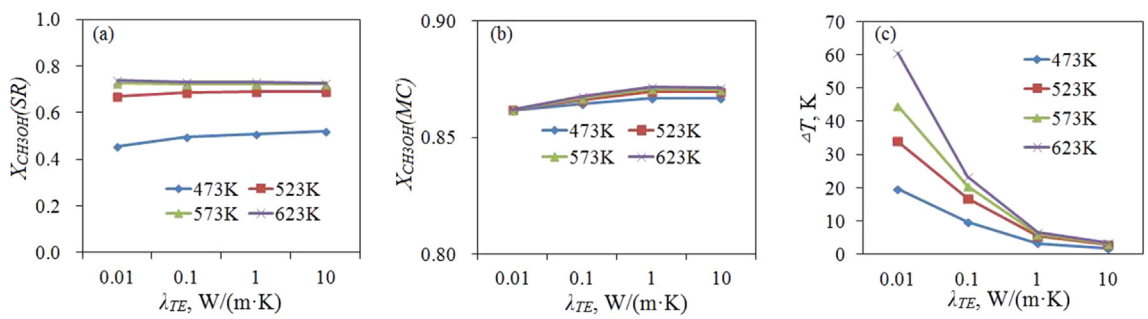

Fig. 11. Variation of methanol conversion X_{CH_3OH} in steam reforming channel and methanol combustion channel (a) and (b) and variation of ΔT with effective thermal conductivity coefficient (c) at different temperatures.

Please cite this article in press as: Wang F, et al., Thermoelectric generation coupling methanol steam reforming characteristic in microreactor, Energy (2014), http://dx.doi.org/10.1016/j.energy.2014.12.019

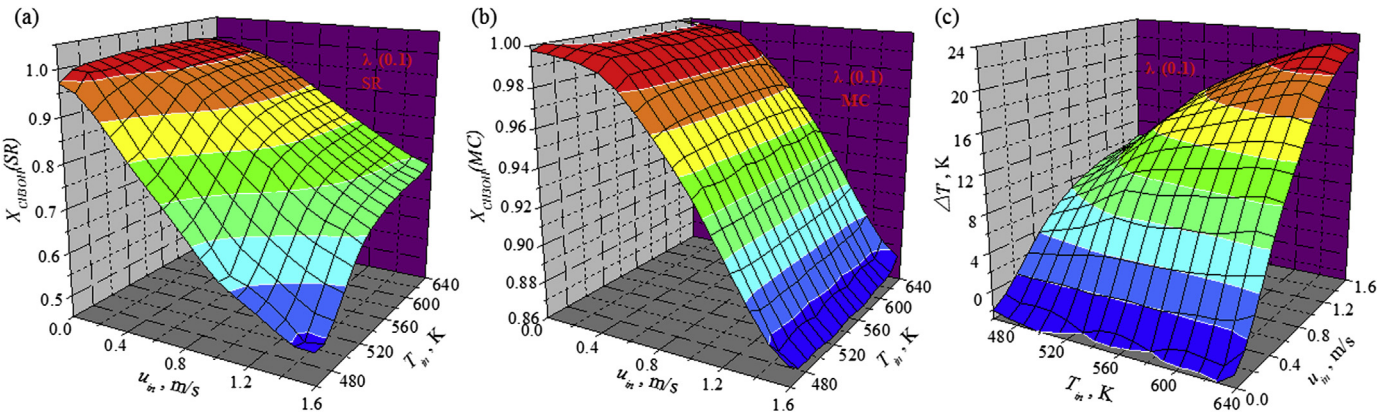

Fig. 12. Variations of methanol conversion in steam reforming channel (a) and methanol combustion channel (b), and variation of largest temperature difference (c) with the inlet velocity and temperature.

quite different from that of the exhausted gas, and even more different from the endothermic reaction of steam reforming. However, the maximum temperature difference $\triangle T$ between the two channel outlets also increases with the inlet velocity. Although the methanol conversion in both reaction channels decreases, the overall amount of the heat consumption and supply increases due to the increasing of the inlet velocity. Temperature differences have also increased since there exists a large thermal resistance between the cold and hot sides of the thermoelectric module and the increment is larger at higher inlet temperatures. With an increase in temperature at both channel inlets, methanol conversion increases and hence ΔT also increases gradually due to the imbalance of the heat supply and consumption. As stated before, reactor performance of the steam reforming for hydrogen production and the performance of the thermoelectric power generator should be considered comprehensively. If the power generation is given a higher priority, the inlet velocity of the reactant should be relatively higher; otherwise, u_{in} should be lower in order to obtain a higher methanol conversion rate.

4.2. Temperature distribution and transport characteristic

As shown in Fig. 13, the temperature distribution of the reactor for hydrogen production that couples the thermoelectric generation model has been analyzed under the conditions of $\lambda_{TE} = 0.1$ W/(m K), $T_{in} = 573$ K and $u_{in} = 1.5$ m/s, with heat source of catalytic combustion. It can be seen that temperature distributions along the surface of the catalytic coating in reforming channel and upper surface of the generator at the reforming side are similar. It is also the similar for the surface of catalytic combustion channel and lower surface of the generator at the heat supply side. Both of them gradually decrease in the fluid flow direction. Also, a uniform temperature difference of about 18 K forms between the cold side and hot side of the thermoelectric generation module, a bit smaller

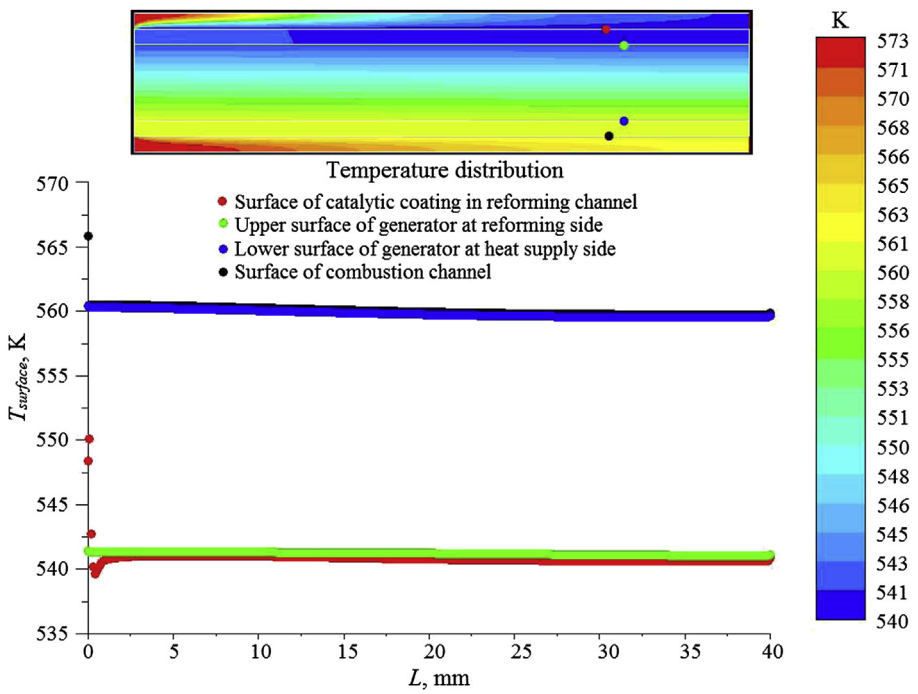

Fig. 13. Temperature contours on the surfaces of methanol steam reforming and catalytic combustion channel, and on the up and down sides of the thermoelectric generation module.

Please cite this article in press as: Wang F, et al., Thermoelectric generation coupling methanol steam reforming characteristic in microreactor, Energy (2014), http://dx.doi.org/10.1016/j.energy.2014.12.019

than that of the exhausted heat supply condition. Therefore, the application of better heat conductors on both sides of the generator model can also obtain a better temperature distribution on the hot and cold ends of the generator. It is also useful for the improvement of hydrogen production performance.

At the very inlet of the steam reforming channel, temperature decreases from 573 K to 540 K rapidly, and it is also lower than that of the upper surface of the generator on the steam reforming side. The cold spot is produced due to the strong endothermic reaction of the methanol steam reforming. Temperature on the catalytic combustion side also drops from 573 K to about of 560 K. This can also be concluded from the heat flux and reaction rate distribution on the surfaces of both channels as shown in Fig. 14, at the conditions of $\lambda(TE) = 0.1$ W/(m K), $u_{in} = 1.5$ m/s, and $T_{in} = 573$ K. Methanol steam reforming reaction rate is a bit larger than that of methanol catalytic combustion reaction, especially at the reactor inlet. Therefore, endothermic steam reforming of methanol is still the dominant reaction in this reactor.

Heat fluxes on the surface of the reforming channel is up to 2464 W/m^2 at the inlet and the heat flux on the corresponding surface of the methanol catalytic combustion channel is up to −2964 W/m^2, both of which are much larger than that of the exhausted gas heating situation. As stated before, effect of heat absorption of the methanol steam reforming is larger than the heat release of the catalytic combustion. Heat energy in coupled process cannot be balanced at local areas, leading to the occurrence of cold spots. So the heat flux value of the inner surfaces of both channels decreases rapidly in the flow direction. The heat fluxes on the reforming channel surface and the catalytic combustion channel surface are also the same in the flow direction. An axial temperature difference also exists in the stainless steel material. Heat fluxes on the upper surface of the generator at the reforming side and the lower surface of the generator on the heat supply side are almost the same. Therefore, it indicates that the stainless steel material functions well in distributing and homogeneously supplying the heat needed.

5. Conclusions

(1) Experimental results of methanol steam reforming for hydrogen production in a micro-reactor with a monolayer catalyst bed show that cold spots occur on the catalyst bed at a high reactant inlet flow rate, which leads to the decreasing of methanol conversion and hydrogen production rates in the products. Maximum temperature differences of the cold spots on the reactor bed and at the reactor entrance are respectively 25 °C and 11 °C at an operation temperature of 220 °C, corresponding to the optimum methanol steam reforming operation temperature based on a copper based catalyst. At a lower reactant inlet flow rate, cold spot effect is not as obvious as that of a high flow rate. Results of this study can be used to optimize the catalyst activity distribution in the reactor for reactions with strong heat effect Strong endothermic steam reforming reaction can also be used to remove the heat on the cold side of a thermoelectric power generator module.

(2) Hydrogen production as well as power generation has been achieved in a reactor that couples methanol steam reforming reaction and thermoelectric generation processes. The strong endothermic reaction can be used for the cold side of the thermoelectric module, with hot air or catalytic methanol combustion being used as heat supply for the hot side of the thermoelectric module. Simulation results with an exhausted gas heat source show that methanol conversion in the reforming channel is influenced mainly by the inlet temperature. However, the temperature difference between the reforming channel and the heating channel is influenced by the thermoelectric material conductivity coefficient. Effects of the inlet velocity on the methanol conversion and temperature difference are on the contrary. Under the catalytic combustion heat source condition, methanol conversion on the steam reforming side is affected mainly by the inlet temperature; however, it is affected mainly by the inlet velocity on the methanol catalytic combustion side.

(3) When the exhausted or waste gas having a low energy density is employed for heating, it is insufficient to provide the needed heat at the reactor inlet, which results in a cold spot at the inlet. To improve the efficiency of both methanol steam reforming and thermoelectric generation, t temperature uniformity on both sides of the thermoelectric generator can be achieved by adopting a high thermal conductivity coefficient metal material. This conclusion is also true for the catalytic combustion heat source condition. The maximum temperature difference between the endothermic and heat supply channels is mainly affected by the thermal conductivity of the module. Effects of inlet velocity on the methanol conversion and maximum temperature difference between the two channels are on the contrary.

(4) Performance test results of the simulated thermoelectric module show that open circuit voltage of the generator increases with ΔT. An output power of 55 mW is achieved for the methanol steam reforming coupled with a single thermoelectric generation module at a temperature difference of 22 K. The corresponding molar fraction of hydrogen can reach about 62.6%, which corresponds to a methanol conversion rate of 72.6%.

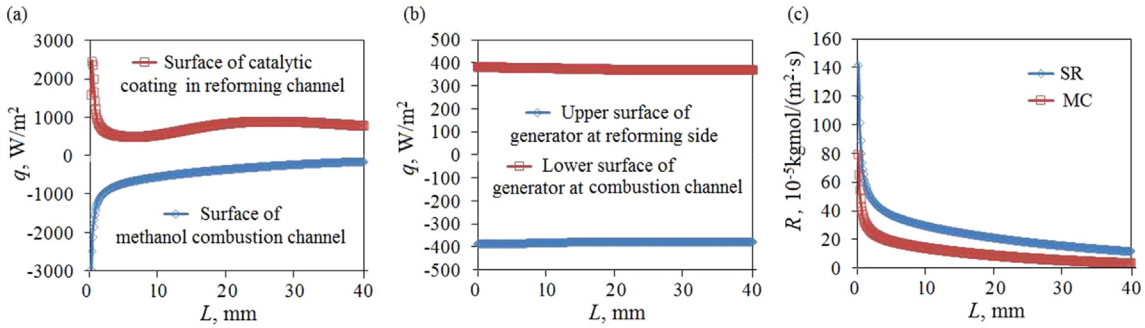

Fig. 14. Heat fluxes on the surfaces of the two channels in the reactor (a), up and down sides of the thermoelectric generation module (b), and reaction rate of steam reforming and methanol catalytic combustion (c).

Please cite this article in press as: Wang F, et al., Thermoelectric generation coupling methanol steam reforming characteristic in microreactor, Energy (2014), http://dx.doi.org/10.1016/j.energy.2014.12.019

Acknowledgements

The authors acknowledge the support of the funding from China Scholarship Council (201208500014) and support of National Natural Science Foundation of China (51006050, 50906104).

References

[1] Chen Wei-Hsin, Liao Chen-Yeh, Hung Chen-I, Huang Wei-Lun. Experimental study on thermoelectric modules for power generation at various operating conditions. Energy 2012;45(1):874–81.
[2] Park. K, Hwang. H.K, Seo. J.W, Seo. W.-S. Enhanced high-temperature thermoelectric properties of Ce- and Dy-doped ZnO for powergeneration [J]. Energy, 54: 139–145.
[3] Champier D, Bedecarrats JP, Rivaletto M, Strub F. Thermoelectric power generation from biomass cook stoves. Energy 2010;35(2):935–42.
[4] Wu Hsin-jay, Chen Sinn-wen, Ikeda Teruyuki, Jeffrey Snyder G. Reduced thermal conductivity in Pb-alloyed $AgSbTe_2$ thermoelectric materials. Acta Mater 2012;60(17):6144–51.
[5] Astrain D, Vián JG, Martínez A, Rodríguez A. Study of the influence of heat exchangers' thermal resistances on a thermoelectric generation system. Energy 2010;35(2):602–10.
[6] Zheng XF, Yan YY, Simpson K. A potential candidate for the sustainable and reliable domestic energy generation–thermoelectric cogeneration system. Appl Therm Eng 2013;53(2):305–11.
[7] Hanamura Katsunori, Kumano Tomoyuki, Iida Yuya. Electric power generation by super-adiabatic combustion in thermoelectric porous element. Energy 2005;30(2–4):347–57.
[8] Liang Gaowei, Zhou Jiemin, Huang Xuezhang. Analytical model of parallel thermoelectric generator. Appl Energy 2011;88(12):5193–9.
[9] Yu Jianlin, Zhao Hua. A numerical model for thermoelectric generator with the parallel-plate heat exchanger. J Power Sources 2007;172(1):428–34.
[10] Hsiao YY, Chang WC, Chen SL. A mathematic model of thermoelectric module with applications on waste heat recovery from automobile engine. Energy 2010;35(3):1447–54.
[11] Wang Guoqiang, Wang Feng, Li Longjian, Zhang Guofu. Experiment of catalyst activity distribution effect on methanol steam reforming performance in the packed bed plate-type reactor. Energy 2013;51:267–72.
[12] Ouzounidou Martha, Ipsakis Dimitris, Voutetakis Spyros, Papadopoulou Simira, Seferlis Panos. A combined methanol autothermal steam reforming and PEM fuel cell pilot plant unit: experimental and simulation studies. Energy 2009;34(10):1733–43.
[13] Chein Reiyu, Chen Yen-Cho, Chung JN. Numerical study of methanol–steam reforming and methanol–air catalytic combustion in annulus reactors for hydrogen production. Appl Energy 2013;102:1022–34.
[14] Du Xiaoze, Shen Yinqi, Yang Lijun, Shi Yingshuang, Yang Yongping. Experiments on hydrogen production from methanol steam reforming in the microchannel reactor. Int J Hydrogen Energy 2012;37(17):12271–80.
[15] Chein Reiyu, Chen Yen-Cho, Chung JN. Axial heat conduction and heat supply effects on methanol-steam reforming performance in micro-scale reformers. Int J Heat Mass Transf 2012;55(11–12):3029–42.
[16] Wang Feng, Zhou Jing, Wang Guoqiang, Zhou Xinjing. Simulation on thermoelectric device with hydrogen catalytic combustion. Int J Hydrogen Energy 2012;37(1):884–8.
[17] Zhou Junhu, Wang Yang, Yang Weijuan, Liu Jianzhong, Wang Zhihua, Cen Kefa. Combustion of hydrogen air in catalytic micro-combustors made of different material. Int J Hydrogen Energy 2009;34(8):35–45.
[18] Roy JP, Mishra MK, Misra Ashok. Parametric optimization and performance analysis of a waste heat recovery system using organic rankine cycle. Energy 2010;35(12):5049–62.
[19] Stijepovic Vladimir Z, Linke Patrick, Stijepovic Mirko Z, Kijevčanin Mirjana Lj, Šerbanović Slobodan. Targeting and design of industrial zone waste heat reuse for combined heat and power generation. Energy 2012;47(1):302–13.
[20] Wang Chaojun, He Boshu, Sun Shaoyang, Wu Ying, Yan Na, Yan Linbo, et al. Application of a low pressure economizer for waste heat recovery from the exhaust flue gas in a 600 MW power plant. Energy 2012;48(1):196–202.
[21] Little Adrienne B, Garimella Srinivas. Comparative assessment of alternative cycles for waste heat recovery and upgrade. Energy 2011;36(7):4492–504.
[22] Chen Yongping, Zhang Chengbin, Wu Rui, Shi Mingheng. Methanol steam reforming in microreactor with constructal tree-shaped network. J Power Sources 2011;196(15):6366–73.
[23] Mei Deqing, Qian Miao, Liu Binhong, Jin Biao, Yao Zhehe, Chen Zichen. A micro-reactor with micro-pin-fin arrays for hydrogen production via methanol steam reforming. J Power Sources 2012;205:367–76.
[24] Pan Minqiang, Wei Xiaoling, Tang Yong. Factors influencing methanol steam reforming inside the oriented linear copper fiber sintered felt. Int J Hydrogen Energy 2012;37(15):11157–66.
[25] Liu Na, Yuan Zhongshan, Wang Congwei, Wang Shudong, Zhang Chunxi, Wang Shujuan. The role of CeO_2–ZrO_2 as support in the ZnO–$ZnCr_2O_4$ catalysts for autothermal reforming of methanol. Fuel Process Technol 2008;89(6):574–81.
[26] Wang Congwei, Liu Na, Pan Liwei, Wang Sheng, Yuan Zhongshan, Wang Shudong. Measurement of concentration profiles over ZnO–Cr_2O_3/CeO_2–ZrO_2 monolithic catalyst in oxidative steam reforming of methanol. Fuel Process Technol 2007;88(1):65–71.
[27] Patel Sanjay, Pant KK. Hydrogen production by oxidative steam reforming of methanol using ceria promoted copper–alumina catalysts. Fuel Process Technol 2007;88(8):825–32.
[28] Chin Ya-Huei, Wang Yong, Dagle Robert A, Shari Li Xiaohong. Methanol steam reforming over Pd/ZnO: catalyst preparation and pretreatment studies. Fuel Process Technol 2003;83(1–3):193–201.
[29] Gonzo Elio E. Hydrogen from methanol-steam reforming. Isothermal and adiabatic monolith reactors' simulation. Int J Hydrogen Energy 2008;33(13):3511–6.
[30] Chen Wei-Hsin, Syu Yu-Jhih. Thermal behavior and hydrogen production of methanol steam reforming and autothermal reforming with spiral preheating. Int J Hydrogen Energy 2011;36(5):3397–408.
[31] Chen Wei-Hsin, Cheng Tsung-Chieh, Hung Chen-I. Numerical predictions on thermal characteristic and performance of methanol steam reforming with microwave-assisted heating. Int J Hydrogen Energy 2011;36(14):8279–91.
[32] Gallucci Fausto, Basile Angelo. Co-current and counter-current modes for methanol steam reforming membrane reactor. Int J Hydrogen Energy 2006;31(15):2243–9.
[33] Ha Ji Won, Kundu Arunabha, Jang Jae Hyuk. Poly-dimethylsiloxane (PDMS) based micro-reactors for steam reforming of methanol. Fuel Process Technol 2010;91(11):1725–30.
[34] Zhang Xinrong R, Shi Pengfei, Zhao Jianxi, Zhao Mengyue, Liu Chuntao. Production of hydrogen for fuel cells by steam reforming of methanol on Cu/ZrO_2/Al_2O_3 catalysts. Fuel Process Technol 2003;83(1–3):183–92.
[35] Sun Zhixin, Gao Lin, Wang Jiangfeng, Dai Yiping. Dynamic optimal design of a power generation system utilizing industrial waste heat considering parameter fluctuations of exhaust gas. Energy 2012;44(1):1035–43.
[36] Domingues António, Santos Helder, Costa Mário. Analysis of vehicle exhaust waste heat recovery potential using a rankine cycle. Energy 2013;49:71–85.
[37] Liu Chao, He Chao, Gao Hong, Xie Hui, Li Yourong, Wu Shuangying, et al. The environmental impact of organic rankine cycle for waste heat recovery through life-cycle assessment. Energy 2013;56:144–54.
[38] Hao Yazhen, Du Xiaoze, Yang Lijun, Shen Yinqi, Yang Yongping. Numerical simulation of configuration and catalyst-layer effects on micro-channel steam reforming of methanol. Int J Hydrogen Energy 2011;36(24):15611–21.
[39] Chein Rei-Yu, Chen Li-Chang, Chen Yen-Cho, Chung JN. Heat transfer effects on the methanol steam reforming with partially filled catalyst layers. Int J Hydrogen Energy 2009;34(13):5398–408.
[40] Lwin Ye, Daud Wan Ramli Wan, Mohamad Abu Bakar, Yaakob Zahira. Hydrogen production from steam–methanol reforming: thermodynamic analysis. Int J Hydrogen Energy 2000;25(1):47–53.
[41] Jiang Yuanli, Huang Qiang, Wang Fuan, Kim Dong Hyun, Lim Mee Sook. Kinetics study of methanol steam reforming over Cu/ZnO/Al_2O_3 catalysts. J Fuel Chem Technol 2001;29(4):347–50.
[42] Pasel Joachim, Emonts Bernd, Peters Ralf, Stolten Detlef. A structured test reactor for the evaporation of methanol on the basis of a catalytic combustion. Catal Today 2001;69:193–200.

Please cite this article in press as: Wang F, et al., Thermoelectric generation coupling methanol steam reforming characteristic in microreactor, Energy (2014), http://dx.doi.org/10.1016/j.energy.2014.12.019